DOI:10.1093/jnci/djt210
Advance Access publication September 21, 2013

ARTICLE

Role of Focal Adhesion Kinase in Regulating YB–1–Mediated Paclitaxel Resistance in Ovarian Cancer

Yu Kang, Wei Hu, Cristina Ivan, Heather J. Dalton, Takahito Miyake, Chad V. Pecot, Behrouz Zand, Tao Liu, Jie Huang, Nicholas B. Jennings, Rajesha Rupaimoole, Morgan Taylor, Sunila Pradeep, Sherry Y. Wu, Chunhua Lu, Yunfei Wen, Jianfei Huang, Jinsong Liu, Anil K. Sood

Manuscript received January 28, 2013; revised May 30, 2013; accepted May 30, 2013.

Correspondence to: Anil K. Sood, MD, Departments of Gynecologic Oncology and Cancer Biology, University of Texas MD Anderson Cancer Center, 1155 Herman Pressler, Unit 1352, Houston, TX 77030 (e-mail: asood@mdanderson.org).

Background We previously found focal adhesion kinase (FAK) inhibition sensitizes ovarian cancer to taxanes; however, the mechanisms are not well understood.

Methods We characterized the biologic response of taxane-resistant and taxane-sensitive ovarian cancer models to a novel FAK inhibitor (VS-6063). We used reverse-phase protein arrays (RPPA) to identify novel downstream targets in taxane-resistant cell lines. Furthermore, we correlated clinical and pathological data with nuclear and cytoplasmic expression of FAK and YB-1 in 105 ovarian cancer samples. Statistical tests were two-sided, and *P* values were calculated with Student *t* test or Fisher exact test.

Results We found that VS-6063 inhibited FAK phosphorylation at the Tyr397 site in a time- and dose-dependent manner. The combination of VS-6063 and paclitaxel markedly decreased proliferation and increased apoptosis, which resulted in 92.7% to 97.9% reductions in tumor weight. RPPA data showed that VS-6063 reduced levels of AKT and YB-1 in taxane-resistant cell lines. FAK inhibition enhanced chemosensitivity in taxane-resistant cells by decreasing YB-1 phosphorylation and subsequently CD44 in an AKT-dependent manner. In human ovarian cancer samples, nuclear FAK expression was associated with increased nuclear YB-1 expression (χ^2 = 37.7; P < .001). Coexpression of nuclear FAK and YB-1 was associated with statistically significantly worse median overall survival (24.9 vs 67.3 months; hazard ratio = 2.64; 95% confidence interval = 1.38 to 5.05; P = .006).

Conclusions We have identified a novel pathway whereby FAK inhibition with VS-6063 overcomes YB-1–mediated paclitaxel resistance by an AKT-dependent pathway. These findings have implications for clinical trials aimed at targeting FAK.

J Natl Cancer Inst;2013;105:1485–1495

Chemotherapy resistance confounds the effective treatment of ovarian and other cancers (1,2). Taxanes are commonly used for treatment of ovarian cancer, but unfortunately most cancers have inherent or acquired resistance (3). To date, the mechanisms by which tumor cells develop resistance to taxanes remain incompletely understood. Early studies showed that taxane resistance is a complex phenomenon (4), and underlying mechanisms are not fully known (5). Thus, new therapeutic approaches are needed to improve the outcome of women with ovarian cancer.

Among the many novel targets, focal adhesion kinase (FAK) is considered to be attractive for therapeutic development (6). FAK is a nonreceptor tyrosine kinase that plays a vital role in many oncogenic pathways (7). Increased FAK expression has been reported in a number of tumor types, including breast, colon, and ovarian cancers (8,9). We and others have previously reported that FAK inhibition can sensitize cancer cells to chemotherapy, but the underlying mechanisms are not well understood (10,11). In this study, we uncovered a novel pathway by which FAK inhibition restores the chemosensitivity of taxane-resistant cells to paclitaxel (PTX) by decreasing YB-1 phosphorylation and nuclear accumulation in an AKT-dependent manner.

Methods

Patient Samples

After approval from the MD Anderson Cancer Center Institutional Review Board, 105 high-grade serous ovarian cancer samples were obtained to construct tissue array as previously described (12). All patients were diagnosed between 1992 and 2011 after primary cytoreductive surgery, and 97% were treated with PTX- and platinum-based adjuvant chemotherapy. Written informed consent was waved because residual samples were used in this study.

Cell Lines and Culture Conditions

The taxane-sensitive (SKOV3ip1 and HeyA8) and taxane-resistant (HeyA8-MDR and SKOV3-TR) human epithelial ovarian cancer cell lines have been described previously (13,14) and were cultured in Roswell Park Memorial Institute 1640 medium supplemented with 10% fetal bovine serum and 0.1% gentamicin sulfate (Gemini Bioproducts, Calabasas, CA) with or without PTX (300 ng/mL for HeyA8-MDR; 150 ng/mL for SKOV3-TR).

Drugs and Reagents

The FAK inhibitor VS-6063 (previously PF-04554878) was obtained from Verastem Inc. (Cambridge, Massachusetts). The sources for all antibodies and reagents are listed in the Supplementary Methods (available online).

In Vitro Gene Silencing

YB-1 small interfering RNA (siRNA) 1 (target sequence 5′-CCUAUGGGCGUCGACCACA-3′) and siRNA2 (target sequence 5′-GUUCCAGUUCAAGGCAGUA-3′) (GenBank Accession numbers: NM_004559) were purchased from Sigma-Aldrich Corporation (Woodland, TX) and used to silence YB-1 expression in the ovarian cancer cell lines. A nonsilencing siRNA that did not share sequence homology with any known human mRNA from a Basic Local Alignment Search Tool (BLAST) search was used as control, as previously described (15,16).

Western Blot Analysis

Lysates from cultured cells was prepared as previously described (10). Typically, 30 μg of protein was fractionated by 10% sodium dodecyl sulfate polyacrylamide gel electrophoresis and transferred to a nitrocellulose membrane (Bio-Rad Laboratories, Hercules, CA). Additional details for immunoblotting are provided in the Supplementary Methods (available online).

Cell Viability, Proliferation, and Apoptosis Assays

Viability [3-(4, 5-dimethylthiazol-2-yl)-2, 5-diphenyltetrazolium bromide (MTT)], proliferation (5-ethynil-2'-deoxyuridine; EdU-Click-it System, Invitrogen, Carlsbad, CA), and apoptosis (annexin-V phycoerythrin [PE]/7AAD staining; BD Biosciences, San Diego, CA) assays were performed as previously described (17).

Animal Experiments

Animal study protocols were approved and supervised by the Institutional Animal Care and Use Committee. To produce tumors, we injected SKOV3ip1, SKOV3-TR (both 1×10^6 cells per 0.2 mL of Hanks' Balanced Salt Solution (HBSS); Life Technologies, Invitrogen), HeyA8, or HeyA8-MDR cells (both 2.5×10^5 cells per 0.2 mL of HBSS) into the peritoneal cavity of the female athymic nude mice (aged 8–12 weeks), which were purchased from the National Cancer Institute–Frederick Cancer Research and Development Center as described previously (13,14). Additional details regarding the treatment schemas are listed in the Supplementary Methods (available online).

Immunohistochemistry

Immunohistochemical analysis for pFAK (Tyr397) and pYB-1 (Ser102) was evaluated using human tissue array samples. For mouse tissues, pFAK (Tyr397), FAK, cleaved caspase 3, Ki67, and collagen staining were evaluated using formalin-fixed, paraffin-embedded tumors. For CD31 staining, sections were done on freshly cut frozen slides. Additional details are provided in the Supplementary Methods (available online).

Reverse-Phase Protein Arrays (RPPAs)

The taxane-resistant (HeyA8-MDR and SKOV3-TR) cells were treated with VS-6063 (1 μM) for 3 hours. Samples were probed with 161 antibodies by RPPA at MD Anderson Cancer Center RPPA Core Facility (see Supplementary Methods, available online, for additional details).

Statistical Analyses

Statistical analyses were performed using the Statistical Package for Social Science software version 18.0 (SPSS, Inc, Chicago, IL). Continuous variables were compared using Student *t* test or analysis of variance. The number of mice per group (n = 10) was chosen as directed by a power analysis to detect a 50% decrease in tumor growth with β error of 0.2. Survival analyses were performed in R version 2.14.2 (R Development Core Team, Vienna, Austria). The patients were grouped according to FAK/YB1 overall score or nuclear expression, respectively. We checked for a relation with overall survival by splitting the samples into high/low or nuclear-positive/nuclear-negative, respectively. The log-rank test was employed to determine the association between FAK/YB1 expression and overall survival. The Kaplan–Meier method was used to generate the survival curves. We computed a statistically significant level for FAK/YB1 and age based on a univariate Cox proportional hazard regression model. Categorical variables were evaluated with Fisher exact test (odds ratio [OR] and 95% confidence interval [CI]).

All statistical tests were two-sided, and a *P* value of less than .05 was considered statistically significant. Additional details are provided in the Supplementary Methods (available online).

Results

Effect of FAK Inhibition on Sensitivity to PTX

We first tested the in vitro effects of VS-6063 on FAK phosphorylation. The expression of pFAK (Tyr397) was statistically significantly inhibited by VS-6063 in a dose-dependent manner in all cell lines (Figure 1A; Supplementary Figure 1A, available online). VS-6063 inhibited pFAK (Tyr397) expression within 3 hours, with a gradual return of expression by 48 hours (Figure 1B; Supplementary Figures 1B and 2, available online). Supplementary Figure 3 (available online) represents a typical experiment in which statistical analysis of triplicate experiments showed no statistically significant changes in FAK phosphorylation at the other residues tested (Tyr 576/577, Tyr 925, or Tyr 861). Because Pyk2 and FAK are approximately 60% identical in the central catalytic domain (18,19), we also tested Tyr402, Tyr 579/580, and Tyr 881 within PYK2. Phosphorylation inhibition of Tyr402 was observed only in the HeyA8 cells, with no phosphorylation residues changed in the HeyA8-MDR cell line after VS-6063 (1 μM) treatment for 1 hour.

VS-6063 as a single agent (0–1 μM) did not affect the growth of any of the cells or their taxane-resistant counterparts (Supplementary Figure 4, available online). However, the combination of PTX and VS-6063 (1 μM) was more effective than either

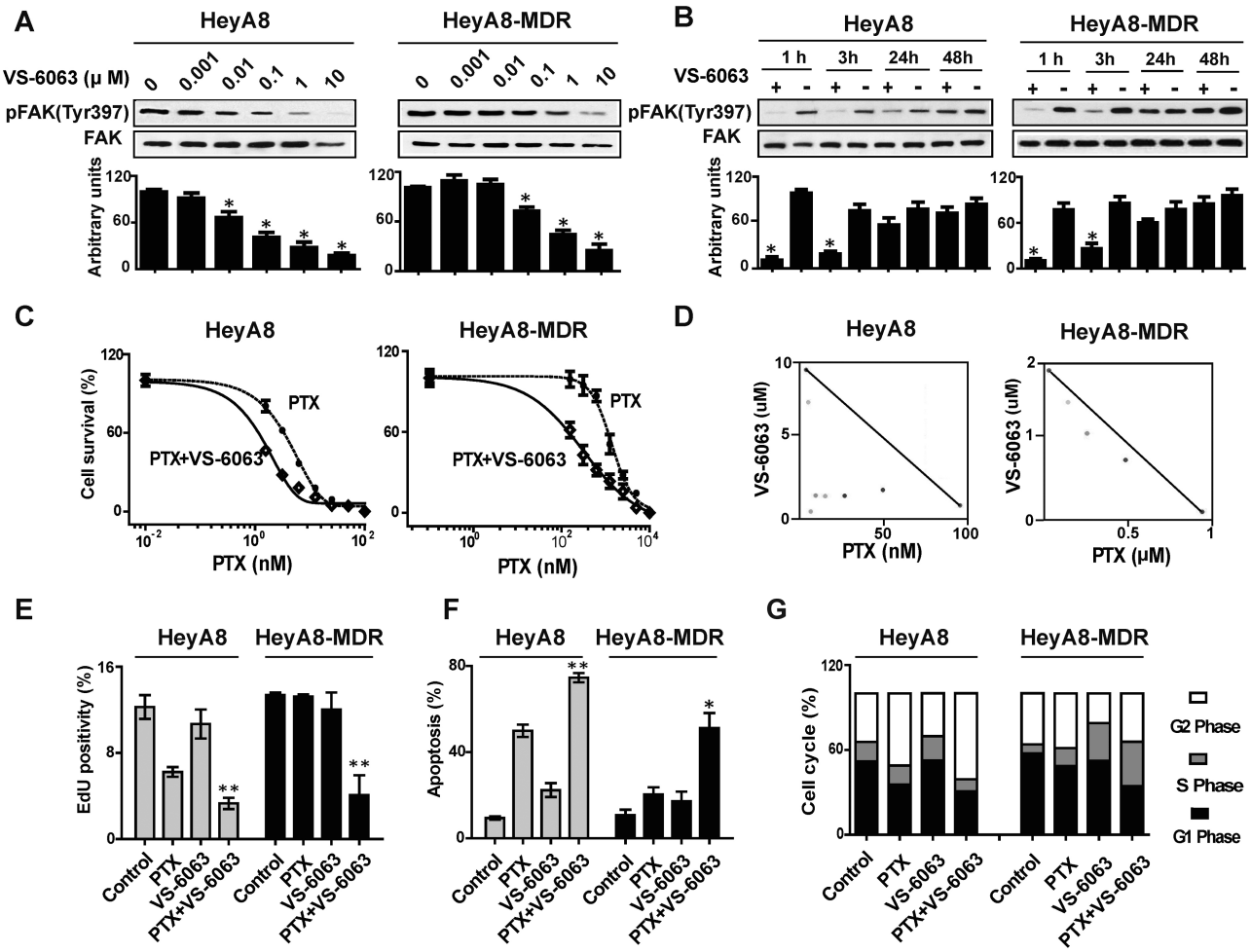

Figure 1. In vitro biological effects of VS-6063 on taxane-sensitive and taxane-resistant cell lines. **A**) Dose-kinetic experiments of the effects of VS-6063 on downregulating FAK phosphorylation. Taxane-sensitive (HeyA8) and taxane-resistant (HeyA8-MDR) cell lines were exposed to increasing doses of VS-6063. Cell lysates were collected and examined by Western blot analysis for pFAK (Tyr397) and total FAK. The immunoblot is shown at the top, and quantification of band intensity relative to total FAK intensity is shown below. Results represent the mean ± standard deviation of triplicate experiments. *$P < .01$, compared with the VS-6063 untreated group. **B**) Time-kinetic experiments of the effects of VS-6063 on downregulating FAK phosphorylation. After cells were treated with 1 μmol/L VS-6063, lysates were collected at 1, 3, 24, and 48 hours and then analyzed for downregulation of pFAK (Tyr397). the immunoblot is shown at the top, and quantification of band intensity relative to total FAK intensity is shown below. Results represent the mean ± standard deviation of triplicate experiments. *$P < .01$, compared with the VS-6063 untreated group. **C**) Cell viability assay of VS-6063 combined with paclitaxel (PTX)–induced cytotoxicity. Cytotoxicity was determined for PTX, both alone (**hatched line**) and in combination with VS-6063 (**solid line**), in HeyA8 and HeyA8-MDR cell lines. Data points indicate the means of three independent experiments. Error bars indicate standard deviation. **D**) Synergy analysis of VS-6063 and PTX in HeyA8 and HeyA8-MDR cell lines. Cells were exposed to different ratios of PTX and VS-6063, and cell viability was assessed using the 3-(4, 5-dimethylthiazol-2-yl)-2, 5-diphenyltetrazolium bromide (MTT) assay. Multiple effect-level isobolograms showed combination data points below, at, and above the isobologram line for a given effect level, indicating synergy, additive effect, and antagonism, respectively. **E**–**G**) Flow cytometric analyses of cell proliferation (**E**), cell apoptosis (**F**), and cell cycle (**G**) in HeyA8 and HeyA8-MDR cell lines treated with VS-6063 and PTX. VS-6063 (1 μM) with or without PTX (at the median inhibitory concentration levels for the taxane-sensitive cell lines) was used to treat HeyA8 and HeyA8-MDR for 72 hours. Columns represent the mean of three independent experiments; error bars indicate standard deviation. *$P < .05$, **$P < .01$, compared with the PTX group. Statistical tests were two-sided, and P values were evaluated using Student t test or analysis of variance.

agent alone. PTX cytotoxicity was 2.1- to 4.9-fold greater in combination with VS-6063 compared with PTX alone (Figure 1C; Supplementary Figure 1C, available online). The combination effect of PTX and VS-6063 was evaluated with combination index by the Chou–Talalay method (20). Interactions between PTX and VS-6063 were synergistic in both HeyA8 and HeyA8-MDR cells (Figure 1D). Simultaneous exposure to doses of PTX and VS-6063 at ratios of 1:1000 for HeyA8 and 1:10 for HeyA8-MDR had a synergistic inhibitory effect on cell growth, with combination index values of 0.953 and 0.705, respectively. No synergy was noted between PTX and VS-6063 in SKOV3ip1 or SKOV3-TR cells, but an additive inhibitory effect on proliferation was noted (data not shown).

Next, we tested the effects of VS-6063 based therapy on proliferation and apoptosis. Compared with PTX alone, the combination of VS-6063 (1 μM) with PTX (at the median inhibitory concentration [IC_{50}] levels of PTX for the SKOV3 and HeyA8 cells of 8.5 and 6.3 nmol/L, respectively) decreased the proliferation rate in both taxane-sensitive and taxane-resistant cells (Figure 1E; Supplementary Figure 1D, available online). For apoptosis, the greatest effects were observed with combined PTX and VS-6063 (Figure 1F; Supplementary Figure 1E, available

online). These findings suggest that VS-6063 in combination with PTX had at least an additive effect on both cell proliferation and apoptosis. PTX increased the proportion of the cell population in the G_2 cell cycle fraction to 51.0% ± 0.4% in the HeyA8 cells compared with control (34.3% ± 0.3%; $P < .001$), and when combined with VS-6063 treatment, the percentage of cells in the G_2 phase statistically significantly increased to 60.8% ± 0.9% ($P < .001$ compared with PTX). HeyA8-MDR cells were not arrested in G_2 phase in either the PTX group or the combination group ($P = .05$) (Figure 1G; Supplementary Figure 1F, available online).

In Vivo Effects of VS-6063

VS-6063 doses of 25 mg/kg twice a day or greater statistically significantly inhibited pFAK (Tyr397) at 3 hours, with return of expression noted by 24 hours (Supplementary Figure 5, available online). Therefore, administration of VS-6063 at 25 mg/kg twice a day was selected as the dosing schedule for subsequent therapy experiments. For therapy experiments, female nude mice bearing HeyA8 tumors in the peritoneal cavity were randomly divided into 4 groups (n = 10 per group): 1) vehicle orally twice daily and phosphate-buffered saline intraperitoneally weekly (control); 2) VS-6063 25 mg/kg orally twice daily; 3) PTX intraperitoneally weekly; and 4) both VS-6063 25 mg/kg orally twice daily and PTX intraperitoneally weekly. There was an 87.4% reduction in tumor weight by PTX monotherapy in the HeyA8 model, and combination therapy resulted in the greatest tumor weight reduction, with a 97.9% reduction ($P = .05$ compared with PTX) (Figure 2, A and B). In the SKOV3ip1 model, a 92.7% tumor weight reduction was observed in the combination group compared with PTX ($P < .001$).

To determine the effect of FAK inhibitor in the chemotherapy-resistant models, we also performed similar in vivo experiments with the HeyA8-MDR and SKOV3-TR cells. Although PTX therapy alone was not effective, VS-6063 treatment resulted in a 42.6% reduction in tumor weight in the HeyA8-MDR model ($P = .41$ compared with control) and a 67.1% reduction in tumor weight in SKOV3-TR model ($P < .001$ compared with control), and the combination of VS-6063 and PTX resulted in greater reduction in tumor growth in HeyA8-MDR (87.2%; $P = .02$) compared with PTX. The combination therapy was statistically superior to PTX in the SKOV3-TR model (91.6%; $P = .04$). No statistically significant differences in feeding behavior or average mouse weights were noted between the treatment groups (Supplementary Figure 6, available online).

To examine potential mechanisms, we assessed therapy effects on angiogenesis (MVD), proliferation (Ki67), and apoptosis (cleaved caspase 3). VS-6063–based combination treatment resulted in decreased pFAK (Tyr397) expression (Figure 2C), reduced MVD (Figure 2D), and proliferation (Figure 2E) and increased apoptosis (Figure 2F). To examine potential effects on the stroma, we performed collagen staining, but there were no statistically significant differences between the treatment groups (Supplementary Figure 7, available online).

Impact of FAK Inhibition on Downstream Signaling

Because FAK is known to signal through beta 1 integrin (21), we first tested whether beta 1 integrin levels were affected by VS-6063, but no statistically significant changes were noted (Supplementary Figure 8, available online). To identify potential signaling pathways downstream of FAK in taxane-resistant cell lines, RPPAs were used and analyzed (DAVID Bioinformatics Resources; http://david.abcc.ncifcrf.gov/). In the VS-6063-treated group, 53 of the 161 proteins analyzed demonstrated a statistically significant change compared with the untreated group in both resistant cell lines ($P < .05$) (Figure 3A; Supplementary Table 1, available online). We found that the AKT pathway was the most involved pathway, including pFAK (Tyr 397), pAKT (Thr308), GSK-3 alpha/beta (Ser21/9), p27(T198), p70S6K (Thr389), PRAS40 (T246), and pYB-1(Ser102). Among these, pYB-1 (Ser102) was the most statistically significantly decreased protein (36.6% decreased by VS-6063 treatment; $P < .001$). Given the potential role of YB-1 in oncogenic and drug-resistance pathways (22,23), we focused on the potential relationship between FAK and YB-1 in subsequent studies.Figure 3B shows that PTX increased nuclear YB-1 expression, whereas PTX combined with VS-6063 decreased its expression in the HeyA8-MDR cells. Immunofluorescence studies also revealed similar findings (Figure 3C).

To determine whether YB-1 plays a role in VS-6063–mediated taxane sensitization, we examined the efficacy of YB-1 siRNA-mediated silencing of endogenous YB-1 (Figure 3D). Figure 3E shows that YB-1 siRNA reduced the PTX IC_{50} from 908.1 nmol/L (95% CI = 710.9 to 1160) to 236.6 nmol/L (95% CI = 204.4 to 273.8) ($P < .001$). YB-1 is a downstream component of the PI3K/AKT signaling pathway (24). Our RPPA data showed that, in the resistant cell lines, VS-6063 markedly decreased AKT and YB-1 phosphorylation (Figure 3A; Supplementary Table 1, available online).

To evaluate the effect of FAK blockade on AKT and YB-1 activation, we measured the levels of AKT and YB-1–phosphorylated proteins by Western blot. In SKOV3-TR cells, we detected decreases in pAKT (Thr308), pAKT (Ser473), and pYB-1 (Ser 102) phosphorylation after treatment with VS-6063 compared with untreated cells, which suggests that the effects of VS-6063 may be mediated by AKT (Figure 4, A and B). Phosphorylation of YB-1 by AKT is required for its translocation from the cytoplasm into the nucleus (24). We, therefore, investigated the effect of a dual AKT1 and AKT2 inhibitor (AKTi) on SKOV3-TR cells. AKTi treatment resulted in a substantial decrease of pYB-1 (Ser102) expression compared with untreated cells in the nucleus (Figure 4C). Also, AKTi decreased translocation of YB-1 into the nucleus, as shown by immunofluorescence analysis (Figure 4D).

As an oncogenic transcription factor, YB-1 can modulate the expression of a variety of downstream targets, including CD44, which is a well-characterized cancer stem cell surface marker of ovarian cancer that contributes, at least in part, to the PTX-resistant phenotype (25). Here, we investigated whether YB-1 is a regulator of CD44 expression in resistant ovarian cancer cells by knocking down YB-1 expression in HeyA8-MDR cells using two siRNA oligonucleotides. As shown in Figure 5A, the protein levels of CD44 were statistically significantly reduced 48 hours after treatment. CD44 expression was downregulated in a time-dependent manner after treatment with VS-6063 (Figure 5B). Moreover, in HeyA8-MDR in vivo experiments, PTX treatment increased the expression of CD44, whereas VS-6063 alone and combination of VS-6063 and PTX resulted in reduced CD44 expression (Figure 5C).

Collectively, in our working model (Figure 5D), under conditions of reduced FAK phosphorylation, AKT is downregulated with

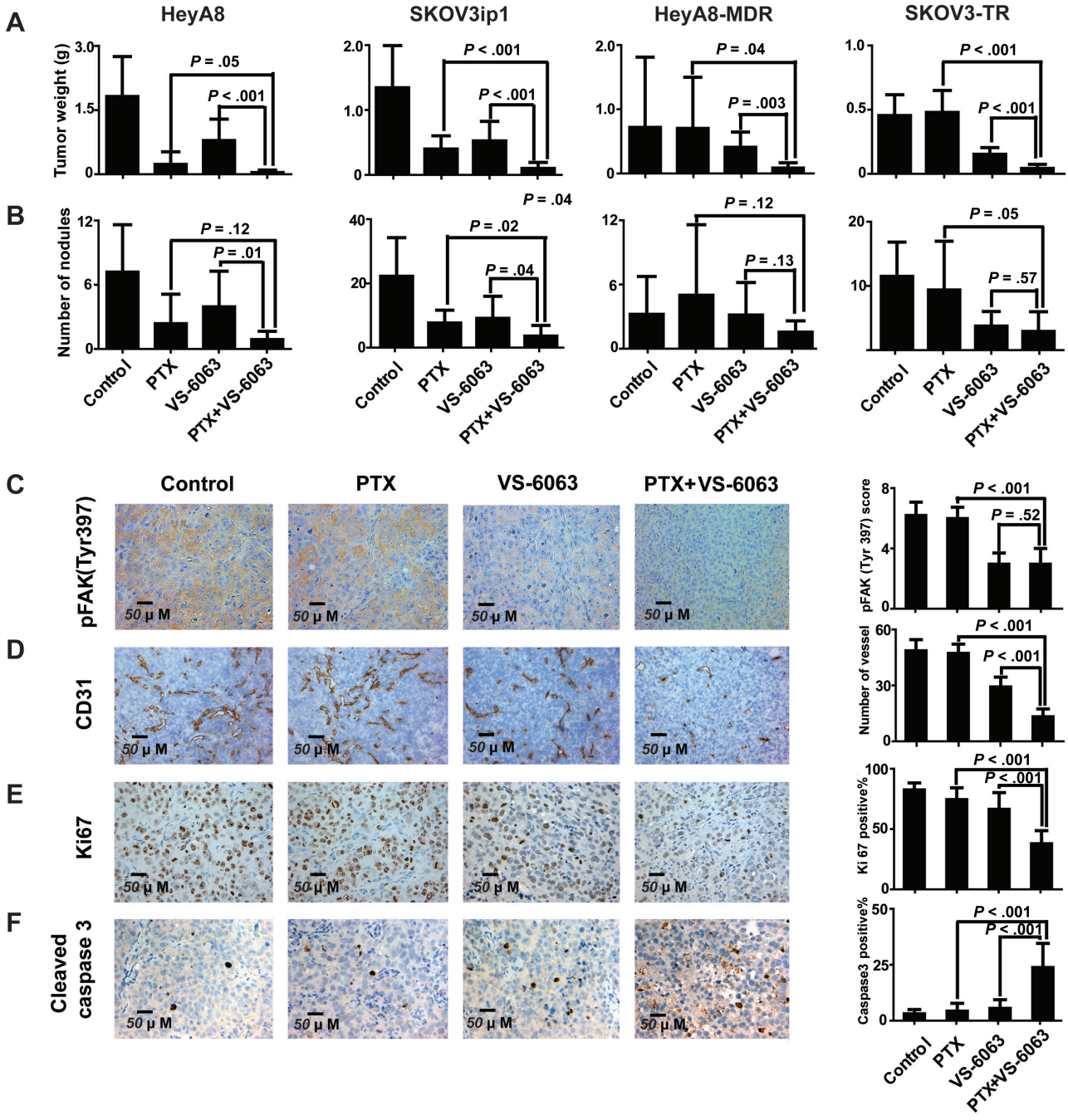

Figure 2. In vivo effects of VS-6063 combined with paclitaxel (PTX). **A** and **B**) Effect of VS-6063 or PTX alone or the combination in PTX-sensitive and PTX-resistant models. Quantification of tumor weights (**A**) and tumor nodules (**B**) in HeyA8, SKOV3ip1, HeyA8-MDR, and SKOV3-TR models with the following: vehicle alone (control), VS-6063 (25 mg/kg orally twice every day), PTX (2 mg/kg for SKOV3ip1 and SKOV3-TR or 2.5 mg/kg for HeyA8 and HeyA8-MDR weekly), or combination VS-6063 plus PTX. Results represent the mean ± standard deviation; n = 10 mice per group. **C**–**F**) Effects of VS-6063 combined with PTX on FAK phosphorylation, angiogenesis, cell proliferation, and apoptosis. HeyA8-MDR tumor samples from each group were stained for pFAK (Tyr397) (**C**), CD31/MVD (**D**), Ki67 (**E**), and cleaved caspase3 (**F**) by immunohistochemistry (scale bar = 50 μm). The bars in the graphs correspond sequentially to the labeled columns of the images at left. Error bars represent standard deviation. Statistical tests were two-sided, and *P* values were evaluated using Student *t* test or analysis of variance.

consequent decreased YB-1 nuclear accumulation and reduced CD44, thereby improving response to PTX.

FAK and YB-1 Coexpression in Ovarian Cancer Samples

To extrapolate the above findings to clinical specimens, we performed immunohistochemical analysis using anti-pFAK (Tyr397) and anti-pYB-1 (Ser102) antibodies on a total of 105 high-grade ovarian serous carcinoma samples. The median age at diagnosis of these patients was 59.7 years (range = 39.1–84.0 years), and the median follow-up was 50.6 months (range = 1.9–119.4 months). Figure 6, A and C, show representative images with low and high immunohistochemical staining for pFAK (Tyr397) and pYB-1 (Ser102). Of the 105 cancer specimens, 40 (38.1%) had high FAK expression and 65 (61.9%) had low or no

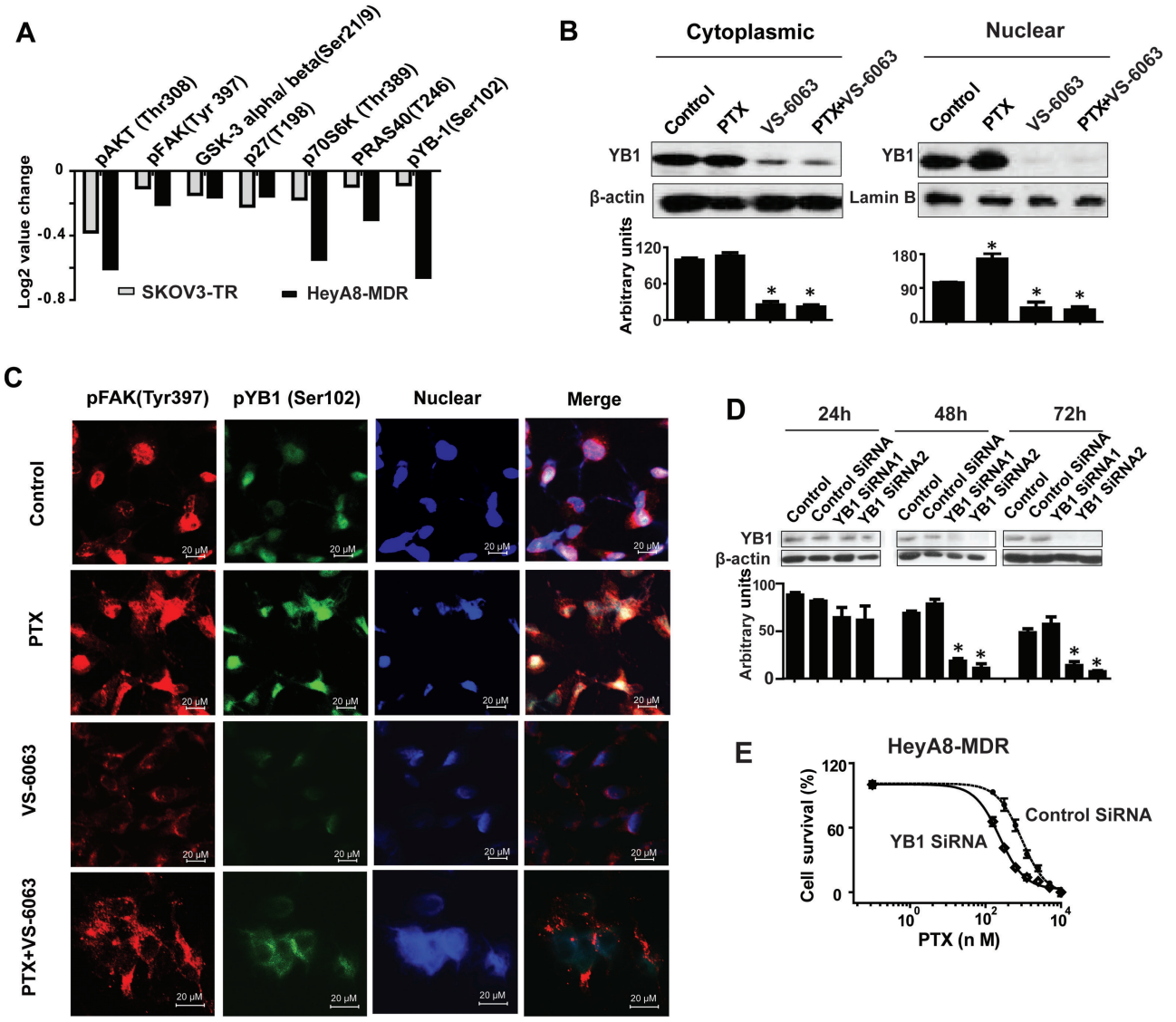

Figure 3. VS-6063 restores YB-1–mediated paclitaxel (PTX) resistance. **A**) Reverse-phase protein arrays (RPPA) of VS-6063–treated taxane-resistant cell lines. Taxane-resistant cell lines (HeyA8-MDR and SKOV3-TR) were treated with 1 μM VS-6063 for 1 hour. RPPA results are presented as the average fold change of seven selected AKT signaling pathway–related proteins in both of the two taxane-resistant cell lines, presented in a bar graph format with normalized natural log2 values. **B**) Western blot analysis of cytoplasmic and nuclear extract proteins collected 48 hours after treatment of HeyA8-MDR cells with VS-6063 or/and PTX. β-Actin and lamin B were used as loading controls for cytoplasmic and nuclear extracts, respectively. The bar graphs show densitometry results. Results were confirmed with triplicate experiments. Error bars indicate standard deviation.. Statistical tests were two-sided, and *P* values were evaluated using Student *t* test. **P* <.05 compared with control group. **C**) Immunofluorescence staining of pFAK (Tyr 397) and pYB-1 (Ser 102) of HeyA8-MDR cells treated with VS-6063 and/or PTX (at the median inhibitory concentration levels for HeyA8) for 48 hours. **D**) Western blot analysis of whole-cell lysates collected 24 to 72 hours after transfection with either control or YB-1–targeted small interfering RNA (siRNA; 2 different sequences). The bar graph shows densitometry results. Results were confirmed with triplicate experiments. Error bars indicate standard deviation. Statistical tests were two-sided, and *P* values were evaluated using Student *t* test. **P* <.001 compared with control siRNA group. **E**) Cell viability assay of YB-1 silencing on PTX sensitivity in taxane-resistant HeyA8-MDR cells. HeyA8-MDR cells were transiently transfected with control or YB-1–targeting siRNAs for 48 hours before the addition of increasing concentrations of PTX. Cells were then incubated for 72 hours followed by 3-(4, 5-dimethylthiazol-2-yl)-2, 5-diphenyltetrazolium bromide (MTT) assay.

FAK expression (Figure 6B), whereas 22 (21.0%) had high pYB-1 (Ser102) expression and 83 (79.0%) had low or no pYB-1 (Ser102) expression (Figure 6D). Kaplan–Meier curves for overall survival time showed that high tumor expression of FAK and YB-1 were associated with higher ovarian cancer mortality (median survival for patients with high vs low FAK expression = 47.2 vs 67.3 months, hazard ratio [HR] of death from ovarian cancer = 1.74, 95% CI = 1.04 to 2.91, *P* = .05; median survival for patients with high vs low YB-1 expression: 48.5 vs 65 months; HR = 1.86, 95% CI = 1.10 to 3.17, *P* = .02) (Figure 6, B and D; Table 1). There was no association between tumor FAK and YB-1 expression and age or tumor stage (Supplementary Table 2, available online).

Next, we examined whether nuclear FAK and YB-1 expressions were associated with survival of patients (Figure 6, E and G). Of the 105 tumors, 21 (20%) showed FAK expression in the nucleus, whereas 15 tumors (14.3%) showed expression of

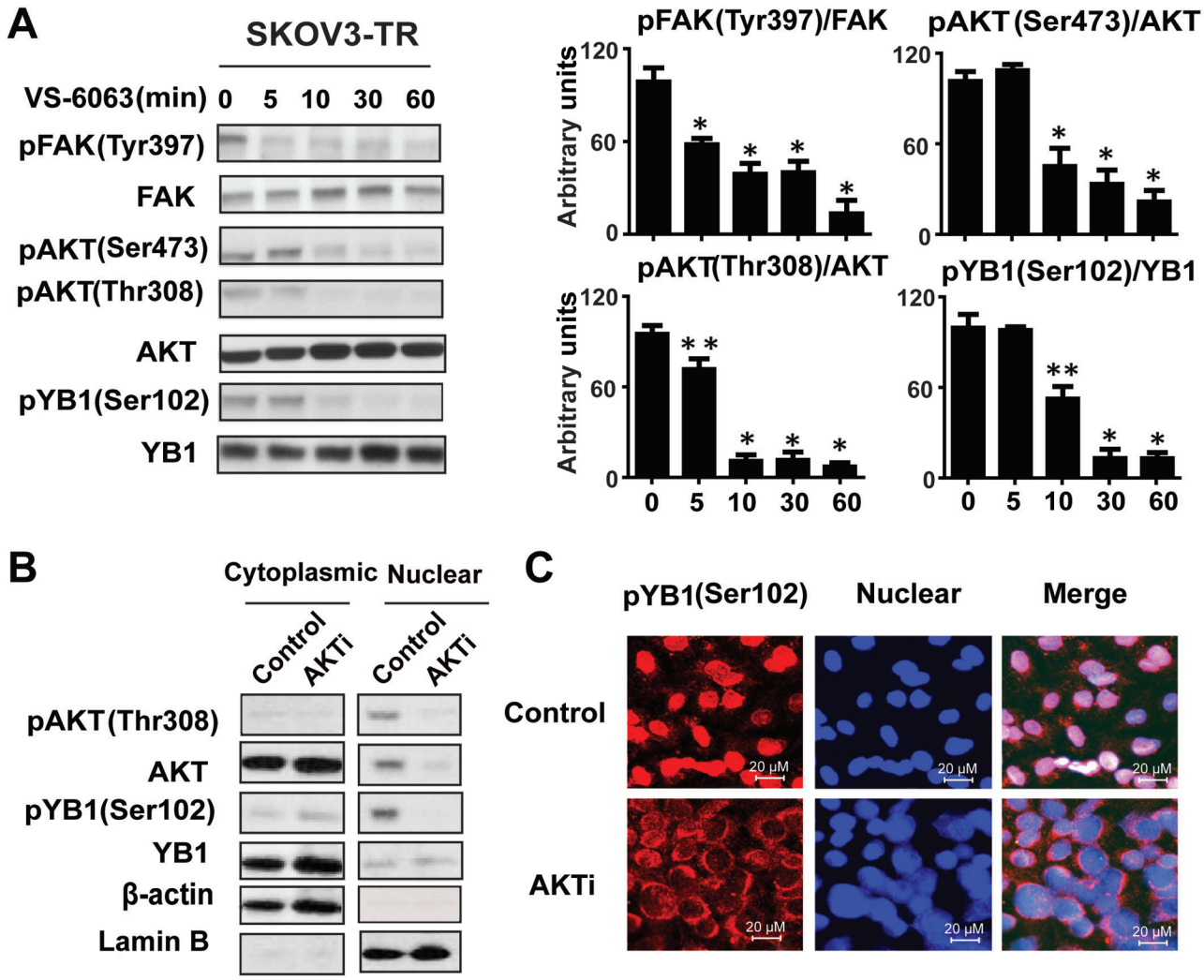

Figure 4. VS-6063 downregulated YB-1 phosphorylation and nuclear translocation in taxane-resistant cells by an AKT-dependent pathway. **A**) Western blot analysis of lysates collected at 0, 5, 10, 30, and 60 minutes after treatment of SKOV3ip-TR cells with VS-6063. The bar graphs at the right show densitometry results. Results were confirmed with triplicate experiments. Error bars indicate standard deviation. Statistical tests were two-sided, and *P* values were evaluated using Student *t* test. **P* <.001 compared with VS-6063 untreated group (time 0); ***P* < .01 compared with VS-6063 untreated group. **B**) Cytoplasmic and nuclear extracts of SKOV3-TR cells were prepared after treatment with AKT1/2 kinase inhibitor (AKTi, 10 μM) for 24 hours, and anti-pYB-1 (Ser 102) and anti-pAKT immunoblots were performed. β-Actin and lamin B were used as loading controls. **C**) Immunofluorescence staining of YB-1 in SKOV3-TR cells. Cells were treated with or without 10 μM AKT 1/2 kinase inhibitor (AKTi) for 24 hours and then fixed, permeabilized, and incubated at 4° C with the primary pYB-1 (Ser 102) antibody and then with the Alexa 594–labeled secondary antibody.

YB-1 in the nucleus. FAK and YB-1 nuclear expressions were also statistically significantly associated with poor overall survival (median survival for patients with FAK nuclear-positive vs nuclear-negative: 47.2 vs 67.3 months, HR = 1.88, 95% CI = 1.06 to 3.36, *P* = .05; YB-1 nuclear-positive vs nuclear-negative: 25.4 vs 67.3 months, HR = 2.41, 95% CI = 1.34 to 4.33, *P* = .005) (Figure 6, F and H; Table 1). Coexpression of nuclear FAK and YB-1 demonstrated a highly statistically significant shortening of overall survival (median survival for patients with nuclear-positive vs nuclear-negative: 24.9 vs. 67.3 months; HR = 2.64; 95% CI =1.38 to 5.05; *P* = .006) (Figure 6 I; Table 1). Tumors with nuclear FAK expression had statistically significantly greater prevalence of increased nuclear YB-1 expression (χ^2 = 37.7; *P* < .001) (Figure 6J).

Discussion

The key findings of this study are that FAK inhibition by VS-6063 enhanced sensitivity of taxane-resistant ovarian cancer cells to PTX both in vivo and in vitro. Moreover, we discovered a novel mechanism by which FAK inhibition overcomes YB-1-mediated PTX resistance by the AKT-dependent pathway.

YB-1 is a member of the cold-shock superfamily and plays a role in multiple biological processes (22) and is overexpressed in a number of cancer types (26–30). Elevated expression of YB-1 protein (especially nuclear YB-1) has been associated with poor patient outcome (31,32) and multidrug resistance (22,23). Furthermore, YB-1 nuclear translocation might be induced in response to various stresses, including chemotherapeutic drugs (33), DNA damage (23), and activation of PI3K-AKT signaling (34). Our in vitro experiments

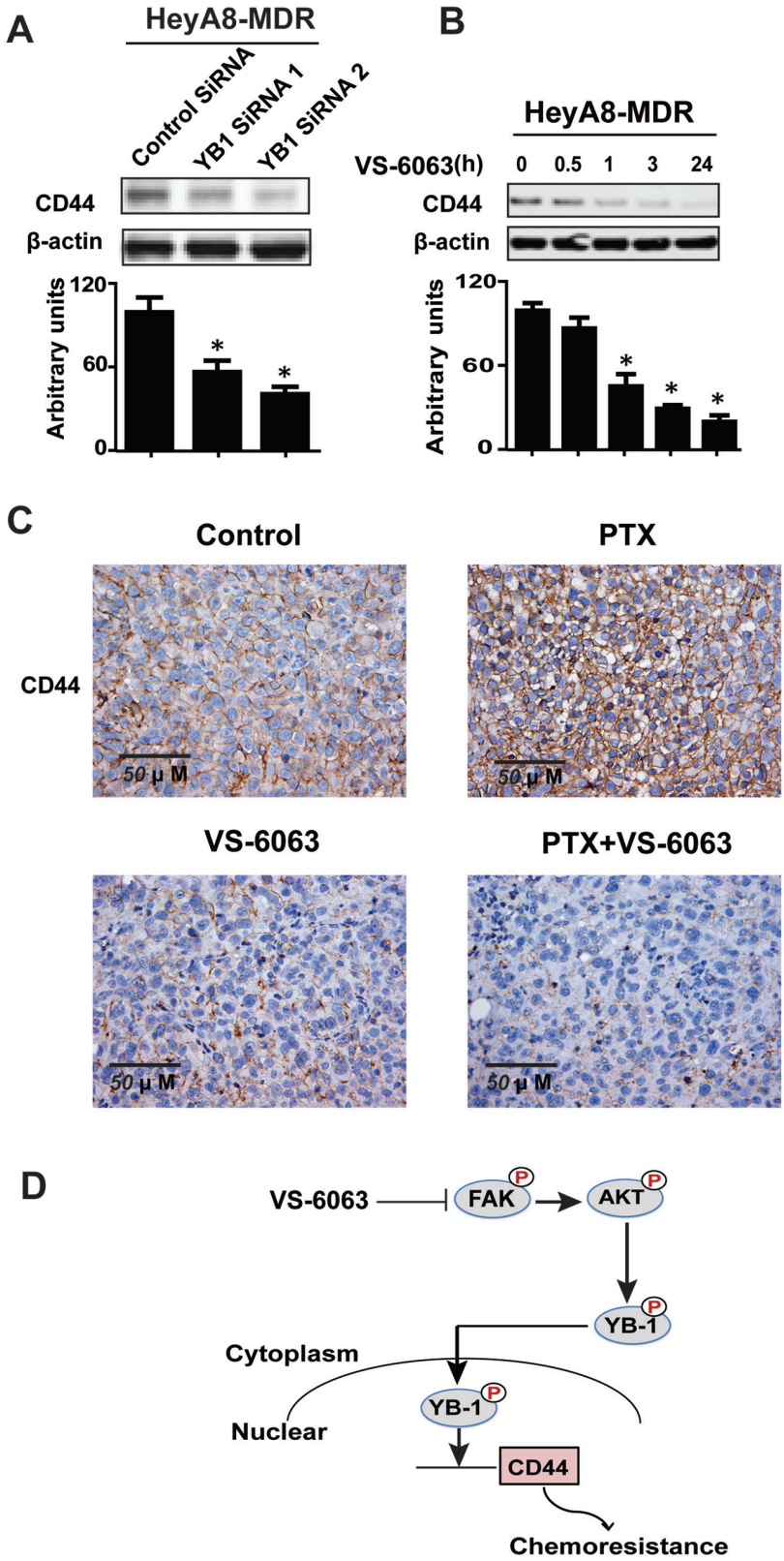

Figure 5. FAK inhibition or silencing of YB-1 downregulates the expression of CD44. **A**) Western blot analysis of lysates collected 48 hours after transfection of HeyA8-MDR cells with either control or one of the two unique YB-1 small interfering RNA (siRNA). CD44 expression was analyzed. β-Actin served as the loading control. The bar graphs show densitometry results. Results were confirmed with triplicate experiments. Error bars indicate standard deviation. Statistical tests were two-sided, and *P* values were evaluated using Student *t* test. **P* < .001 compared with control group. **B**) Western blot analysis of lysates collected 24 hours after VS-6063 treatment of HeyA8-MDR cells. Results were confirmed with triplicate experiments. Error bars indicate standar deviation. Statistical tests were two-sided, and *P* values were evaluated using Student *t* test. **P* < .001 compared with control group. **C**) Immunohistochemical staining of CD44 for HeyA8-MDR tumor samples from each group. **D**) Working model of FAK inhibition in overcoming YB-1–mediated chemoresistance.

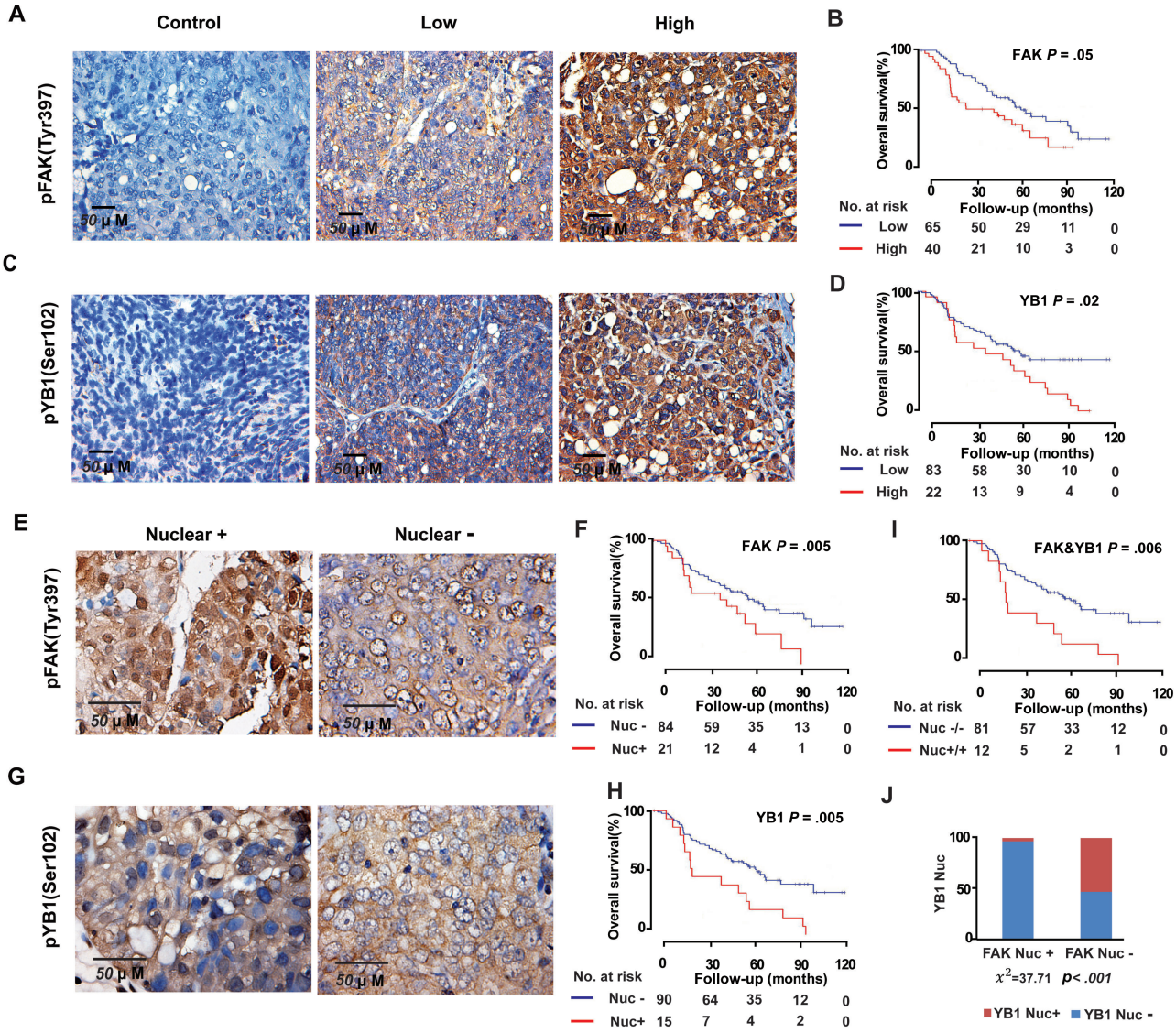

Figure 6. Impact of pFAK (Tyr 397) and pYB-1 (Ser 102) expressions on patient survival. **A**) Representative images of human ovarian tumors with low or high immunohistochemical staining for pFAK (Tyr 397). pFAK (Tyr 397) and pYB-1 (Ser 102) expressions were dichotomized into low (overall score of 0–5) and high (overall score of 6–8) groups for analysis. Overall score was obtained by adding the assigned values for intensity (range = 0–4) and percentage of tumor cells (range = 0–4). Negative control represents a sample of ovarian cancer tissue used in this study processed for immunohistochemistry with the secondary antibody alone. Immunohistochemistry staining of cell nuclei (**blue**) and pFAK (Tyr 397) (**brown**) are represented in the images. **B**) Kaplan–Meier curves of disease-specific mortality for patients whose ovarian tumors expressed high and low levels of pFAK (Tyr 397). The log-rank test (2-sided) was used to compare differences between the two groups. **C**) Representative images of human ovarian tumors with low and high immunohistochemical staining for pYB-1 (Ser 102). **D**) Kaplan–Meier curves of disease-specific mortality for patients whose ovarian tumors expressed high and low levels of pYB-1 (Ser 102). **E** and **G**) Representative images of human ovarian cancer nuclear-positive or nuclear-negative for pFAK (Tyr 397) (**E**) and pYB-1 (Ser 102) (**G**). **F**, **H**, and **I**), Kaplan–Meier curves of disease-specific mortality of patients whose ovarian tumor expressed nuclear-positive vs nuclear-negative expression of pFAK (Tyr 397) (**F**), pYB-1 (Ser 102) (**H**), and coexpression (**I**). **J**) Fisher exact test (2-sided) showed pFAK (Tyr 397) nuclear expression was strongly associated with pYB-1 (Ser 102) nuclear expression levels.

showed that PTX promoted nuclear translocation of YB-1 in the resistant cell lines. FAK inhibition with VS-6063 provided an effective approach to overcome the YB-1–mediated PTX resistance.

Although FAK is a cytoplasmic protein, recently it has been found to have novel functions in the nucleus. One of the nuclear functions of FAK might be direct interaction with p53 (35), promoting cell proliferation and survival through enhanced p53 degradation (36). However, given the high rate of p53 mutations in ovarian cancer (37), we hypothesized that modulation of YB-1 might be another mechanism involved in the nuclear functions of FAK. Co-Immunoprecipitation (Co-IP) of FAK and YB-1 showed no direct binding (data not shown). AKT binds to YB-1 and phosphorylates it on the cold-shock domain (34) and regulates the nuclear translocation of YB-1 (24). Our study showed that AKT and YB-1 were inactivated in response to VS-6063 treatment. YB-1 has been reported to bind to the promoters of EGFR, ABCB1, and some stem cell–related genes, which can contribute to drug resistance (CD44 and CD49f) (15). Among these, CD44 plays a key

Table 1. Univariate analysis of independent prognostic factors in patients with high-grade serous ovarian cancer (n = 105)

Variable	HR (95% CI)*	*P*†
Increased age	1.07 (0.64 to 1.77)	.80
pFAK(Y397) expression (high vs low)	1.74 (1.04 to 2.91)	.05
pYB-1(Ser102) expression (high vs low)	1.86 (1.10 to 3.17)	.02
Nuclear pFAK(Y397) (nuclear-positive vs nuclear-negative)	1.88 (1.06 to 3.36)	.05
Nuclear pYB-1(Ser102) (nuclear-positive vs nuclear-negative)	2.41 (1.34 to 4.33)	.005
Nuclear pFAK(Y397) and pYB-1(Ser102) (nuclear-positive vs nuclear-negative)	2.64 (1.38 to 5.05)	.006

* CI = confidence interval; HR=hazard ratio of death from ovarian cancer.

† Two-sided, *P* value obtained from Cox proportional hazards regression model.

role in many oncogenic functions (38) and is considered a potential marker for cancer stem cells (25,39–41). To clinically evaluate the therapeutic benefit of targeting cancer stem cells through FAK inhibition, a phase I/Ib study of paclitaxel in combination with VS-6063 in patients with advanced ovarian cancer is ongoing (http://clinicaltrials.gov/ct2/show/NCT01778803).

Although our findings provide a new understanding of FAK's role in chemoresistance in ovarian cancer, some potential limitations should be considered. Whether the mechanism presented here is present in other tumor types is not known and will require additional work. Moreover, whether FAK inhibitors can effectively sensitize paclitaxel-resistant or paclitaxel-refractory tumors in clinical settings is also not known and will need to be tested in clinical trials. Nevertheless, we have uncovered a novel pathway by which FAK inhibition restores sensitivity of taxane-resistant cells to PTX by decreasing YB-1 phosphorylation and nuclear accumulation, and its downstream target gene-CD44. Future clinical studies should include mechanism-based pharmacodynamics studies to determine the biologically active doses in humans.

References

1. Bookman MA. First-line chemotherapy in epithelial ovarian cancer. *Clin Obstet Gynecol*. 2012;55(1):96–113.
2. Luqmani YA. Mechanisms of drug resistance in cancer chemotherapy. *Med Princ Pract*. 2005;14(Suppl 1):35–48.
3. Markman M. Taxanes in the management of gynecologic malignancies. *Expert Rev Anticancer Ther*. 2008;8(2):219–226.
4. Yusuf RZ, Duan Z, Lamendola DE, Penson RT, Seiden MV. Paclitaxel resistance: molecular mechanisms and pharmacologic manipulation. *Curr Cancer Drug Targets*. 2003;3(1):1–19.
5. Murray S, Briasoulis E, Linardou H, Bafaloukos D, Papadimitriou C. Taxane resistance in breast cancer: mechanisms, predictive biomarkers and circumvention strategies. *Cancer Treat Rev*. 2012;38(7):890–903.
6. Golubovskaya VM. Focal adhesion kinase as a cancer therapy target. *Anticancer Agents Med Chem*. 2010;10(10):735–741.
7. Schwock J, Dhani N, Hedley DW. Targeting focal adhesion kinase signaling in tumor growth and metastasis. *Expert Opin Ther Targets*. 2010;14(1):77–94.
8. Cance WG, Harris JE, Iacocca MV, et al. Immunohistochemical analyses of focal adhesion kinase expression in benign and malignant human breast and colon tissues: correlation with preinvasive and invasive phenotypes. *Clin Cancer Res*. 2000;6(6):2417–2423.
9. Sood AK, Coffin JE, Schneider GB, et al. Biological significance of focal adhesion kinase in ovarian cancer: role in migration and invasion. *Am J Pathol*. 2004;165(4):1087–1095.
10. Halder J, Kamat AA, Landen CN, Jr., et al. Focal adhesion kinase targeting using in vivo short interfering RNA delivery in neutral liposomes for ovarian carcinoma therapy. *Clin Cancer Res*. 2006;12(16):4916–4924.
11. Halder J, Landen CN, Jr., Lutgendorf SK, et al. Focal adhesion kinase silencing augments docetaxel-mediated apoptosis in ovarian cancer cells. *Clin Cancer Res*. 2005;11(24 Pt 1):8829–8836.
12. Rosen DG, Huang X, Deavers MT, et al. Validation of tissue microarray technology in ovarian carcinoma. *Mod Pathol*. 2004;17(7):790–797.
13. Thaker PH, Han LY, Kamat AA, et al. Chronic stress promotes tumor growth and angiogenesis in a mouse model of ovarian carcinoma. *Nat Med*. 2006;12(8):939–944.
14. Halder J, Lin YG, Merritt WM, et al. Therapeutic efficacy of a novel focal adhesion kinase inhibitor TAE226 in ovarian carcinoma. *Cancer Res*. 2007;67(22):10976–10983.
15. Lu C, Han HD, Mangala LS, et al. Regulation of tumor angiogenesis by EZH2. *Cancer Cell*. 2010;18(2):185–197.
16. Merritt WM, Lin YG, Spannuth WA, et al. Effect of interleukin-8 gene silencing with liposome-encapsulated small interfering RNA on ovarian cancer cell growth. *J Natl Cancer Inst*. 2008;100(5):359–372.
17. Nick AM, Stone RL, Armaiz-Pena G, et al. Silencing of p130cas in ovarian carcinoma: a novel mechanism for tumor cell death. *J Natl Cancer Inst*. 2011;103(21):1596–1612.
18. Lev S, Moreno H, Martinez R, et al. Protein tyrosine kinase PYK2 involved in Ca(2+)-induced regulation of ion channel and MAP kinase functions. *Nature*. 1995;376(6543):737–745.
19. Sasaki H, Nagura K, Ishino M, et al. Cloning and characterization of cell adhesion kinase beta, a novel protein-tyrosine kinase of the focal adhesion kinase subfamily. *J Biol Chem*. 1995;270(36):21206–21219.
20. Chou TC. Drug combination studies and their synergy quantification using the Chou-Talalay method. *Cancer Res*. 2010;70(2):440–446.
21. Shibue T, Weinberg RA. Integrin beta1-focal adhesion kinase signaling directs the proliferation of metastatic cancer cells disseminated in the lungs. *Proc Natl Acad Sci U S A*. 2009;106(25):10290–10295.
22. Kohno K, Izumi H, Uchiumi T, Ashizuka M, Kuwano M. The pleiotropic functions of the Y-box-binding protein, YB-1. *Bioessays*. 2003;25(7):691–698.
23. Sorokin AV, Selyutina AA, Skabkin MA, et al. Proteasome-mediated cleavage of the Y-box-binding protein 1 is linked to DNA-damage stress response. *EMBO J*. 2005;24(20):3602–3612.
24. Basaki Y, Hosoi F, Oda Y, et al. Akt-dependent nuclear localization of Y-box-binding protein 1 in acquisition of malignant characteristics by human ovarian cancer cells. *Oncogene*. 2007;26(19):2736–2746.
25. Zhang S, Balch C, Chan MW, et al. Identification and characterization of ovarian cancer-initiating cells from primary human tumors. *Cancer Res*. 2008;68(11):4311–4320.
26. Stratford AL, Habibi G, Astanehe A, et al. Epidermal growth factor receptor (EGFR) is transcriptionally induced by the Y-box binding protein-1 (YB-1) and can be inhibited with Iressa in basal-like breast cancer, providing a potential target for therapy. *Breast Cancer Res*. 2007;9(5):R61.
27. Gimenez-Bonafe P, Fedoruk MN, Whitmore TG, et al. YB-1 is upregulated during prostate cancer tumor progression and increases P-glycoprotein activity. *Prostate*. 2004;59(3):337–349.
28. Shibahara K, Sugio K, Osaki T, et al. Nuclear expression of the Y-box binding protein, YB-1, as a novel marker of disease progression in non-small cell lung cancer. *Clin Cancer Res*. 2001;7(10):3151–3155.

29. Shibao K, Takano H, Nakayama Y, et al. Enhanced coexpression of YB-1 and DNA topoisomerase II alpha genes in human colorectal carcinomas. *Int J Cancer*. 1999;83(6):732–737.
30. Kamura T, Yahata H, Amada S, et al. Is nuclear expression of Y box-binding protein-1 a new prognostic factor in ovarian serous adenocarcinoma? *Cancer*. 1999;85(11):2450–2454.
31. Bargou RC, Jurchott K, Wagener C, et al. Nuclear localization and increased levels of transcription factor YB-1 in primary human breast cancers are associated with intrinsic MDR1 gene expression. *Nat Med*. 1997;3(4):447–450.
32. Yahata H, Kobayashi H, Kamura T, et al. Increased nuclear localization of transcription factor YB-1 in acquired cisplatin-resistant ovarian cancer. *J Cancer Res Clin Oncol*. 2002;128(11):621–626.
33. Fujita T, Ito K, Izumi H, et al. Increased nuclear localization of transcription factor Y-box binding protein 1 accompanied by up-regulation of P-glycoprotein in breast cancer pretreated with paclitaxel. *Clin Cancer Res*. 2005;11(24 Pt 1):8837–8844.
34. Sutherland BW, Kucab J, Wu J, et al. Akt phosphorylates the Y-box binding protein 1 at Ser102 located in the cold shock domain and affects the anchorage-independent growth of breast cancer cells. *Oncogene*. 2005;24(26):4281–4292.
35. Golubovskaya VM, Cance WG. FAK and p53 protein interactions. *Anticancer Agents Med Chem*. 2011;11(7):617–619.
36. Lim ST, Chen XL, Lim Y, et al. Nuclear FAK promotes cell proliferation and survival through FERM-enhanced p53 degradation. *Mol Cell*. 2008;29(1):9–22.
37. Integrated genomic analyses of ovarian carcinoma. *Nature*. 2011;474(7353):609–615.
38. Naor D, Wallach-Dayan SB, Zahalka MA, Sionov RV. Involvement of CD44, a molecule with a thousand faces, in cancer dissemination. *Semin Cancer Biol*. 2008;18(4):260–267.
39. Du L, Wang H, He L, et al. CD44 is of functional importance for colorectal cancer stem cells. *Clin Cancer Res*. 2008;14(21):6751–6760.
40. Leung EL, Fiscus RR, Tung JW, et al. Non-small cell lung cancer cells expressing CD44 are enriched for stem cell-like properties. *PLoS One*. 2010;5(11):e14062.
41. Al-Hajj M, Wicha MS, Benito-Hernandez A, Morrison SJ, Clarke MF. Prospective identification of tumorigenic breast cancer cells. *Proc Natl Acad Sci U S A*. 2003;100(7):3983–3988.

Funding

Portions of this work were supported by the National Institutes of Health (CA 109298, P50 CA083639, P50 CA098258, CA128797, RC2GM092599); the Ovarian Cancer Research Fund, Inc. (Program Project Development Grant); Cancer Prevention and Research Institute of Texas (RP110595); the Department of Defense (OC073399, W81XWH-10-1-0158, BC085265); the Zarrow Foundation; the Marcus Foundation; the Blanton-Davis Ovarian Cancer Research Program; and the Betty Anne Asche Murray Distinguished Professorship. BZ was supported by NCI-DHHS-NIH T32 Training Grant (T32 CA101642). NCI institutional Core Grant CA16672.

Note

The study sponsors had no role in design of the study; the collection, analysis, and interpretation of the data; the writing of the manuscript; and the decision to submit the manuscript for publication.

We thank Dr Robert Langley and Donna Reynolds for assistance with immunohistochemistry. We thank Michael Worley and the Department of Scientific Publications for editing the manuscript. We also thank Verastem, Inc. for providing the FAK inhibitor VS-6063.

Affiliations of authors: Department of Gynecologic Oncology and Reproductive Medicine (YK, WH, CI, CVP, HJD, BZ, TL, JH, NBJ, RR, MT, TM, SP, SYW, CL, YW, AKS), Center for RNAi and Non-Coding RNA (CI, AKS), Department of Pathology (JH, JL), and Department of Cancer Biology (AKS), The University of Texas MD Anderson Cancer Center, Houston, TX; Shanghai Key Laboratory of Female Reproductive Endocrine Related Diseases, Hospital and Institute of Obstetrics and Gynecology, Shanghai Medical College of Fudan University, Shanghai, China (YK); Department of General Surgery, Union Hospital, Tongji Medical College, Huazhong University of Science and Technology, Wuhan, Hubei, China (TL).